Coastal Dynamics 2017
Paper No. 102

REDUCTIONS IN BERM HEIGHT AND FORESHORE SLOPE DUE TO SEAWARD FLOW ORIGINATED FROM FILTRATION ON GRAVEL BEACH

Toshinori Ishikawa[1], Takaaki Uda[2], Masumi Serizawa[3], Mitsunaga Okamoto[4], Yasuhito Noshi[5] and Shiho Miyahara[3]

Abstract

The closure mechanism of the mouth of a floodway owing to the deposition of gravel by waves was investigated, taking the Shin-nakagawa floodway flowing into the Fuji coast as an example. A movable bed experiment with a model scale of 1/50 using a two-dimensional wave channel was carried out, while changing the discharge of the floodway. It was found that the berm height and foreshore slope were reduced by the seaward flow originated from filtration on the gravel beach. A model for predicting beach changes was proposed based on the contour-line-change model. The effect of seaward flow on the cross-shore sand transport was incorporated in the model, and the calculation results were in good agreement with the experimental results. The model was further applied to the calculation of the 3-D bathymetric changes caused by the surface flow associated with a flood of the Shin-nakagawa floodway. The measured and predicted results agreed well.

Key words: filtration, seaward flow, gravel beach, berm height, equilibrium slope, experiment, contour-line-change model

1. Introduction

In a floodway for a drainage extending across sandy beaches exposed to the open sea, the mouth of the floodway is often closed by sand deposition due to waves. On these coasts, a high berm develops in general because of a large incident wave height, and this causes the full closure of the mouth of the floodway. At the Shin-nakagawa floodway flowing into the Fuji coast, the floodway is successfully maintained even though high waves are often incident during storms. The field observation of this floodway showed that reductions in berm height and foreshore slope were assumed to occur under the condition that seaward flow originated from filtration exists, and this is supposed to be a mechanism of the drainage free from maintenance. Such effect, however, has not yet been investigated. In addition to the field observation of the Shin-nakagawa floodway, a movable-bed experiment with a scale of 1/50 using a two-dimensional wave channel was carried out. As a result, it was suggested that the foreshore slope and berm height could be decreased with the increase in the amount of discharge from the floodway, as an effect of the seaward flow to the cross-shore sand transport. Such effect could be explained by the mechanism that the equilibrium slope of sand, which is determined by the balance between the intensities of outgoing and incoming waves (Serizawa et al. 2003), decreases under the condition that waves and seaward flow coexist. In this study, a model for predicting beach changes was developed, taking the effect of the seaward flow originated from filtration into account using the contour-line-change model proposed by Serizawa et al. (2003), and numerical simulation results were compared with those obtained by the experiment. Furthermore, the model was applied to the calculation of the 3-D bathymetric changes around the Shin-nakagawa floodway caused by the surface flow associated with a flood. Part of this study was published in the Proceedings of 35th ICCE (Uda et al. 2016).

[1]Public Works Research Center, Japan. ishikawa@pwrc.or.jp
[2]Head, Shore Protection Research, Public Works Research Center, Japan. uda@pwrc.or.jp
[3]Coastal Engineering Laboratory Co., Ltd., Japan. coastseri@nifty.com
[4]Numazu Public Works Office, Shizuoka Prefecture, Japan. mitsunaga1_okamoto@pref.shizuoka.lg.jp
[5]Nihon University, Japan. noshi.yasuhito@nihon-u.ac.jp

2. Observation at Shin-nakagawa Floodway

Figure 1 shows the satellite image of the Shin-nakagawa floodway on the Fuji coast. This floodway is composed of old and new floodways on the east and west sides, respectively, with a horseshoe or rectangular mouth, and they extend obliquely to the direction normal to the shoreline. In Fig. 1, a stream flowing from the mouth of the old floodway can be observed on the east side with a pond in front of the mouth, and this pond has been completely closed by a sand bar of 12 m width, and no channel connects between the pond and the sea. A discharge of approximately 0.8 m^3/s continuously flowed down to the sea during the day, implying that all the drainage from the floodway discharged as the seaward flow owing to filtration across the sand bar. On the other hand, in front of the floodway, a slightly concave shoreline is observed, and this might closely be related to the seaward flow owing to filtration crossing the sand bar. Therefore, in the field observation, this point was investigated in detail.

Figure 2 shows the detailed condition of the floodways. The old floodway faces approximately normal to the shoreline, whereas the new one extends normal to the direction of the old floodway. A large amount of gravel was deposited in front of the new floodway, and almost half of the mouth was buried with gravel. In front of the old floodway, the drainage from the floodway rapidly filtrated into the gravel layer near the mouth. Here, the elevation of the mouth is +0.34 m above the mean sea level (MSL). As typical wave conditions of storm waves with a probability of occurrence of once a year on this coast, the significant wave height $H_{1/3}$ ranges between 2 and 3 m and the wave period $T_{1/3}$ is 11 s.

Figure 1. Satellite image of Shin-nakagawa floodway taken on January 9, 2015.

Figure 2. Horseshoe and rectangular mouths of old and new Shin-nakagawa floodways, respectively, and deposition of gravel in front of the mouths.

Figure 3 shows the old floodway and the pond formed in front of the mouth. The drainage from the old floodway flowed eastward, and then all discharge filtrated into the gravel layer. Although a high berm **A** was formed immediately east of the old floodway, the south side of this berm was truncated by the steep slope **B** of the angle of repose of gravel, which was formed by the erosion on the side slope by strong currents during a flood. A berm was formed in front of the old floodway, but the height of the berm was much smaller than the berm height on the nearby beach. Figure 4 shows the shoreline where the water filtrated from the pond in front of the old floodway flows out to the sea. In the vicinity of this location, a concave shoreline was formed together with an upward concave profile of the beach face. This is in good agreement with the fact that a concave shoreline was observed in front of the floodway, as shown in Fig. 1. Figure 5 shows the beach material deposited in front of the old floodway, and the beach was composed of gravel of grain size ranging between 5 and 10 cm.

Figure 3. Mouth of old floodway and a pond in front of the mouth.

Figure 4. Concave shoreline where filtration water flows out into sea.

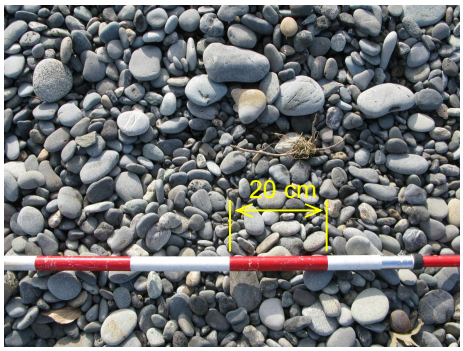

Figure 5. Grain size of beach material composing berm.

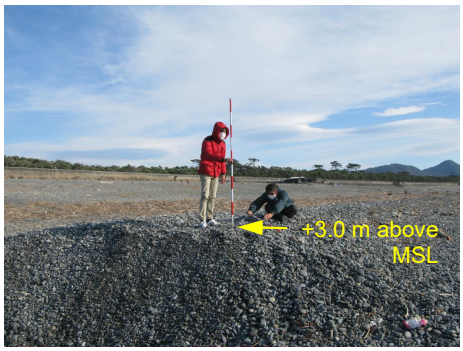

Figure 6. Berm height of 3 m above MSL immediately east of the floodway.

Figure 7. Berm height of 2.1 m above MSL in front of the mouth of old floodway.

Figure 8. Foreshore slope of 1/2.5 at natural beach.

In the field observation, the berm height and foreshore slope were measured in the vicinity of the floodway. First, the berm height immediately east of the floodway was +3 m above MSL, as shown in Fig. 6, whereas that in front of the old floodway was +2.1 m, as shown in Fig. 7, i.e., 0.9 m lower than the berm height of the natural sandy beach. As for the foreshore slope, the slope was 1/2.5 immediately west of the old floodway (Fig. 8). In contrast, the foreshore slope at a location where filtration flow discharged out to the sea was 1/4 (Fig. 9), and thus the reduction of the foreshore slope was confirmed. Furthermore, strong seaward flow was observed in the central part of a concave shoreline, as shown in Fig. 10, as in the case near the apex of the beach cusps (Shibasaki et al. 2004), and a reduction in the height of the incoming

waves was observed because of strong seaward flow concentrated at the central part. Finally, it was confirmed that the berm height and foreshore slope were reduced at a location with seaward flow originated from filtration on the gravel beach, resulting in the formation of a concave shoreline, as mentioned above. In reference to the concept of the equilibrium slope as described by Serizawa et al. (2003), the seaward flow is assumed to intensify the action of outgoing waves, resulting in the reduction of the beach slope. Thus, seaward flow originated from filtration on the gravel beach is assumed to decrease in equilibrium slope, and beach changes occur so that the foreshore slope and berm height are reduced.

Figure 9. Foreshore slope of 1/4 at a location where filtration water discharges out to sea.

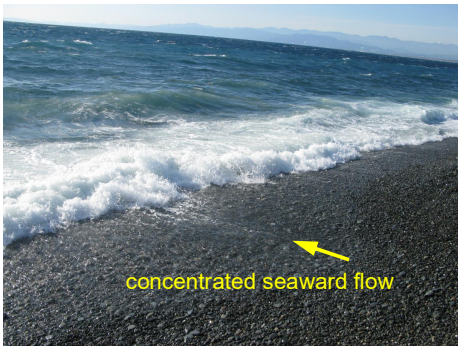

Figure 10. Concentrated seaward flow associated with filtration.

3. Method of Experiment

A two-dimensional movable bed experiment was carried out to investigate the mechanism of the reductions in berm height and foreshore slope observed at the Shin-nakagawa floodway. A wave tank of 8 m length, 0.4 m width and 35 cm depth was used for the experiment, and a model beach with the initial slope of 1/5 was produced using gravel with the median diameter d_{50} of 3.3 mm. By setting the model scale as 1/50, regular waves became incident to the model beach. Variables were determined so as to satisfy Froude′s similarity. Meshes at 10 cm intervals were drawn on the side glass of the wave channel, as shown in Fig. 11, and the longitudinal profile was measured by photographing from the side glass.

In a small-scale experiment, characteristic beach changes occur, and the type of profile changes can be classified, depending on the C-parameter proposed by Horikawa (1988), using the grain size d of sand, the wave height H, the wave period T and the beach slope $\tan\beta$.

$$H_o/L_o = C\,(\tan\beta)^{-0.27}\,(d/L_o)^{0.67} \tag{1}$$

In Eq. (1), sand is considered to be transported shoreward to form a berm if C is smaller than 4, whereas seaward sand transport dominates and the foreshore will be eroded if C is greater than 8. In this study, sand deposition in front of the floodway mouth is important, and thus the condition in which shoreward sand transport is predominant was adopted. Regular waves were employed in the experiment.

First, as a preliminary test of the beach changes, the wave condition for the berm height to be 6 cm (3 m in the prototype) was tested, and a wave height of 3 cm and a wave period of 1.3 s were selected. This experimental condition corresponds to the waves of H = 1.5 m and T = 9.2 s in the prototype. Furthermore, the duration of the experiment was determined to be 3 h, because the berm has sufficiently developed after a 3-hour wave generation. Table 1 shows the experimental conditions.

In the experiment, a model floodway of 10 cm width and made of acrylic resin was installed along the side wall of the wave channel, and the longitudinal profile was measured on the side glass by tracing the profile. When the mouth of the floodway is set at the shoreline, a large amount of sand is deposited, and thus the mouth was set back by 50 cm (25 m in the prototype) from the shoreline landward of the berm top. The elevation of the basement of the floodway was set to be 4.5 cm below MSL. The discharge of the floodway was kept constant using a water pump. Figure 12 shows the side view and overview of the wave

tank. A constant discharge was given under the wave condition in which a berm height of 6 cm is reproduced. As the discharge in the experiment, Q_m = 17 l/min in the experiment (Q_p = 0.3 m^3/s in the prototype) was selected as the reference discharge, and Q_m was increased at six steps, as shown in Table 1. In addition, the inner water level behind the berm was measured using the photographs.

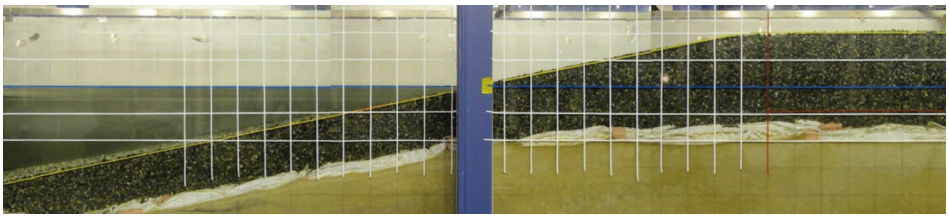

Figure 11. Wave flume and initial beach profile.

Table 1. Conditions of experiment.

Facility	Two-dimensional wave tank: 8 m length, 0.4 m width and 0.35 cm depth
Method of experiment	Movable bed experiment: reproduction of berm height of 6 cm
Model scale	1/50
Duration of experiment	3 hrs
Wave conditions	Regular waves: H_m = 3 cm, T_m = 1.3 s (H = 1.5 m and T = 9.2 s in the prototype)
Discharge (Q_m)	Case 1: 0 ml/s, Case 2: 17 ml/s, Case 3: 34 ml/s, Case 4: 68 ml/s, Case 5: 102 ml/s, Case 6: 136 ml/s, Case 7: 170 ml/s
Grain size	Median diameter d_{50} = 3.3 mm.
Model beach	Movable bed: Initial slope of 1/5
Model floodway	Acrylic resin: 30 cm length, 10 cm width and 7.1 cm height Elevation of the basement of the floodway: 4.5 cm below MSL

(a) Side view

(b) Overview

Figure 12. Side view and overview of wave tank.

4. Results of Experiment

Given a constant discharge from the floodway, waves were incident to the model beach of uniform slope. With the increase in water level in front of the mouth, seaward flow owing to filtration on the gravel beach occurred because of the difference between the inner water level and the mean sea level. Because the width of the floodway is one-fourth of the channel width, the effect of the seaward flow owing to filtration on the beach changes concentrated along the side wall, where the mouth was set, and its effect decreases with increasing distance from the side wall, suggesting the formation of a concave topography. In the experiment, therefore, the longitudinal profile along the side wall where the most dominant effect could be observed was measured. Although a two-dimensional wave tank was employed in this experiment, the floodway model was placed within 1/4 width of the channel. Therefore, 3-D beach changes may occur in

the channel associated with not only cross-shore sand transport but also longshore sand transport.

Figure 13 shows the results of the experiment on berm formation with the existence of seaward flow owing to filtration and the change in longitudinal profile after a three-hour wave action in Cases 1, 3, 5, and 7, as well as the inner water level in front of the floodway. In Case 1 with no discharge, shoreward sand transport took place under the waves, and a berm of 6.2 cm height along with a foreshore slope of 1/1.8 was formed. This result gives a reference to other cases. In Case 3 with the discharge of Q_m = 34 ml/s, the berm height was 5.9 cm and the foreshore slope was 1/1.8; the berm height was reduced by 0.3 cm relative to that in Case 1, but there was no change in the foreshore slope. In Case 5 with the discharge of Q_m = 102 ml/s, the berm height was 5.2 cm, which decreased by 1.0 cm. In addition, the foreshore slope became as gentle as 1/2.4. Finally, in Case 7 with Q_m = 170 ml/s, the berm height was 4.0 cm lower than that in Case 1 by 2.2 cm and the gentle foreshore slope of 1/2.5 was formed. Thus, it was found experimentally that the berm height and foreshore slope decreased with the increase in discharge. Table 2 shows all the measured results.

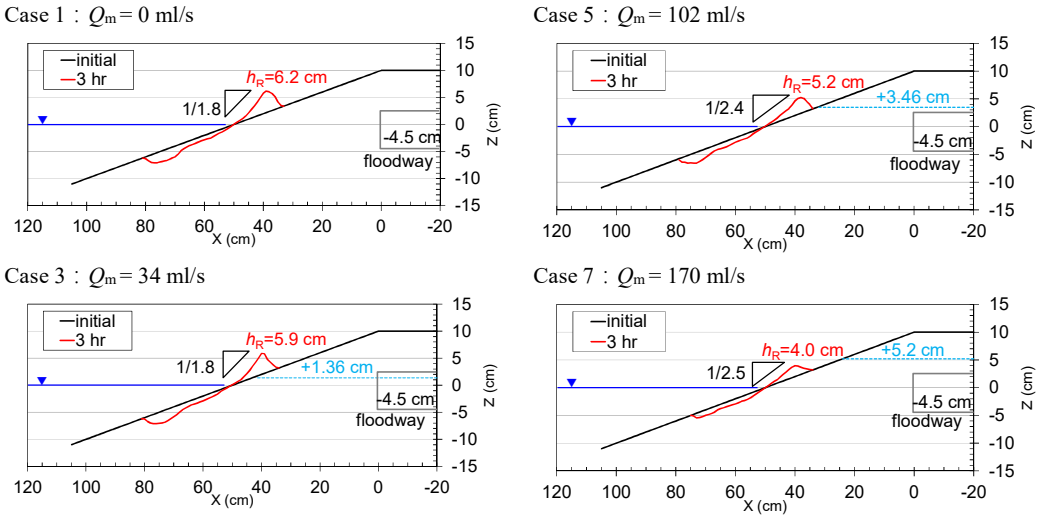

Figure 13. Longitudinal profiles in Cases 1, 3, 5, and 7 after 3-hour wave action.

Table 2. Results of experiment.

Case	Discharge Q_m (ml/s)	cotβ	berm height h_R (cm)	h_R/h_{R1}	Inner water level W_L (cm)
1	0	1.8	6.2	1	-
2	17	1.7	5.8	0.93	0.97
3	34	1.8	5.9	0.95	1.36
4	68	1.9	5.7	0.92	2.50
5	102	2.4	5.2	0.84	3.46
6	136	2.3	5.3	0.86	4.60
7	170	2.5	4.0	0.64	5.20

Figure 14 shows the relationship between the discharge Q_m (ml/s) and the inner water level W_L (cm) on the basis of the experimental results, as shown in Table 2. A relation was obtained.

$$W_L = 0.033\ Q_m \tag{2}$$

W_L increased with the discharge, and the increase in the inner water level in turn intensified the seaward flow owing to filtration on the gravel layer. Figure 15 shows the relationship between the discharge Q_m and the ratio of the berm height h_R relative to that in Case 1 (h_R/h_{R1}). Between the two variables, a relation was

obtained:

$$h_R/h_{R1} = 1.0\text{-}0.0016\ Q_m \tag{3}$$

The berm height gradually decreased with the increase in the amount of discharge. Furthermore, the relationship between the reciprocal of the foreshore slope and the discharge Q_m is shown in Fig. 16 with the linear relation

$$\cot\beta = 1.79 + 0.004\ Q_m \tag{4}$$

The foreshore slope and the berm height decrease with increasing Q_m, and these results are in good agreement with the observation results around the Shin-nakagawa floodway.

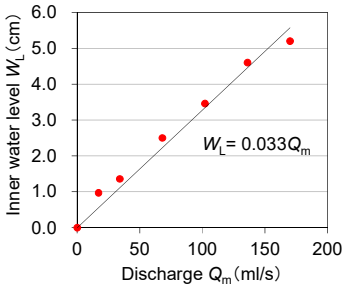

Figure 14. Relationship between Q_m and inner water level W_L.

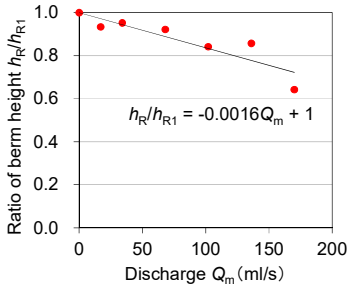

Figure 15. Relationship between Q_m and ratio of berm height relative to that in Case 1 (h_R/h_{R1}).

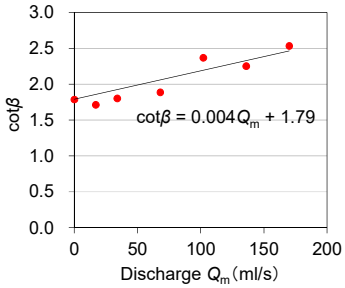

Figure 16. Relationship between Q_m and reciprocal of foreshore slope, cotβ.

5. Numerical Model

The cross-shore sand transport under the condition that waves and seaward flow coexist was derived. The cross-shore sand transport q_z is assumed to be given as a linear sum of the component due to waves, q_{zW}, and that due to seaward flow, q_{zR}, as Eq. (5).

$$q_z = q_{zw} + q_{zR} \tag{5}$$

Here, shoreward sand transport was assumed to be positive, and for the cross-shore sand transport q_z, the basic equation in the contour-line-change model proposed by Serizawa et al. (2003) was employed, as in Eq. (6).

$$q_{zW} = A_W \cdot \left(\frac{\cot\beta}{\cot\beta_C} - 1 \right) \quad \left(-h_C \le z \le h_R \right) \tag{6}$$

$$A_W = \varepsilon(z) \cdot K_z \cdot (EC_g)_b \cdot \sin\beta_C \tag{7}$$

Here, β is the angle of the seabed slope, β_c is the angle of the equilibrium slope, z is the seabed level of each contour line, h_c is the depth of closure, and h_R is the berm height. Beach changes can occur in the depth zone between h_c and h_R. The coefficient A_w given by Eq. (7) shows the intensity of sand transport due to waves and is proportional to the wave intensity. $\varepsilon(z)$ is the depth distribution function of the intensity of cross-shore and longshore sand transport, and in this study, we employed the depth distribution proposed by Uda and Kawano (1996) as Eq. (8).

$$\varepsilon(z)=\begin{cases}=\dfrac{2}{h_c^3}\left(\dfrac{h_c}{2}-z\right)(z+h_c)^2 & (-h_c\le z\le h_R)\\ =0 \qquad (z<-h_c\ ,h_R<z)\end{cases} \tag{8}$$

Furthermore, K_z is the coefficient of cross-shore sand transport, and $(EC_g)_b$ is the energy flux of waves at the breaking point. By referring to the expression of the sand transport component due to waves as Eq. (6) and designating the sand transport component due to the seaward flow q_{zR} as - A_R, we obtain

$$q_{zR}=-A_R \qquad (A_R>0) \tag{9}$$

Here, Eq. (5) can be transformed to Eq. (10) using Eqs. (6) and (9).

$$q_z = A'\cdot\left(\frac{\cot\beta}{\cot\beta_c'}-1\right) \tag{10}$$

$$A'=\lambda A_w \tag{11}$$

$$\cot\beta_c'=\lambda\cot\beta_c \tag{12}$$

$$\lambda=1+A_R/A_w \tag{13}$$

Although Eq. (10) is similar to Eq. (6), the intensity of the sand transport and the equilibrium slope change as Eqs. (11) and (12) in response to the factor λ as Eq. (13). Without the seaward flow ($A_R = 0$), λ is unity, and Eq. (10) agrees with Eq. (6). On the other hand, when the action due to the seaward flow is intensified compared with that due to waves (larger A_R/A_W), λ takes a greater value than unity, and the equilibrium slope $\tan\beta_c$' ($1/\cot\beta_c$') decreases with a larger coefficient of intensity of sand transport (A'). The effect of the seaward flow on the cross-shore sand transport can be incorporated in this way as the change in equilibrium slope. In the calculation, we assumed that $\lambda = 1$ in a wave-dominated field, and the condition of $\lambda > 1$ was set when seaward flow is dominant, using the numerical model of the contour-line-change model as proposed by Serizawa et al. (2003). In this method, $\cot\beta_c$ and the intensity of sand transport A_W are increased by λ using Eqs. (12) and (11) where seaward flow dominates, and the numerical simulation considering the effect of seaward flow could be possible. λ is an additional correction factor.

To predict 3-D beach changes, we need the equation of longshore sand transport rate, q_x, and here the same equation in the contour-line-change model (Serizawa et al. 2003) as in Eq. (14) was employed

$$q_x=\varepsilon(z)\cdot K_x\cdot(EC_g)_b\cos\alpha_b\sin\alpha_b \tag{14}$$

Here, K_x is the coefficient of longshore sand transport, and α_b is the breaker angle. The calculation domain was discretized using the staggered meshes, and the sand transport rate was calculated using the cross-shore sand transport of Eq. (10) and the longshore sand transport of Eq. (14). The beach changes were calculated explicitly by solving the continuity equation of Eq. (15) by the explicit finite-difference method.

$$\frac{\partial Y}{\partial t}=-\frac{\partial q_x}{\partial x}-\frac{\partial q_z}{\partial z} \tag{15}$$

Here, $Y(x, z, t)$ is the offshore distance from the x-axis to the location of each contour line and t is time.

Table 3. Calculation conditions.

Numerical model	Contour-line change model (Serizawa et al. 2003)
Initial bathymetry	Straight, parallel contours with a slope of 1/5
Equilibrium slope	1/1.8 (Z = 10-0 cm), 1/3.6 (Z = 0-15 cm)
Wave conditions	Breaker height H_b = 3.0 cm
Depth of closure and berm height	Depth of closure h_c = 6 cm, Berm height h_R = 6.2 cm h_c = 5 cm and h_R = 4.0 cm (X = 0-10 cm) in Case 7
Coefficients of sand transport	Coefficient of longshore sand transport K_y = 0.2, Coefficient of cross-shore sand transport $K_z = 0.1K_y$
Depth distribution of sand transport	Cubic equation given by Uda and Kawano (1996)
Critical slope of falling sand	1/2 on land and seabed
Calculation range in depth	z = 10.5 - -15.5 cm
Calculation mesh	ΔX = 5 cm, ΔZ = 1 cm
Time intervals	Δt = 0.0001 h
Boundary conditions	q_x = 0 at landward and seaward boundaries, and q_y = 0 at both ends
Remarks	Additional correction factor in Case 7: $\lambda = 1+A_R/A_W$ = 1.4 (X = 0-10 cm, Z = +4 - -5 cm)

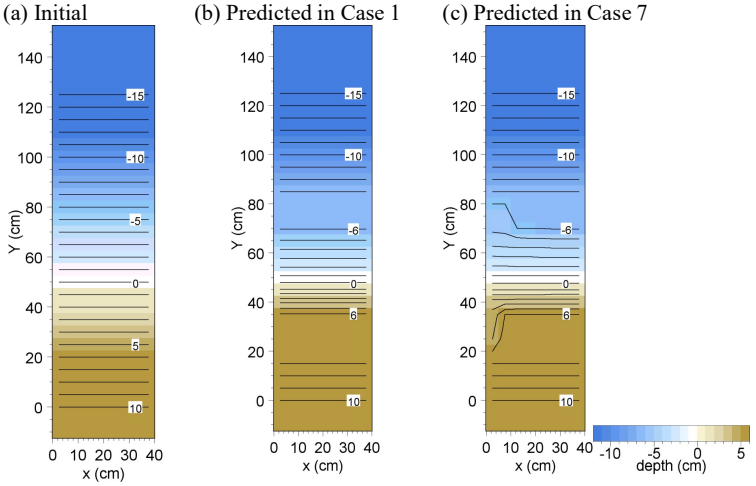

Figure 17. Bathymetric changes in Cases 1 and 7.

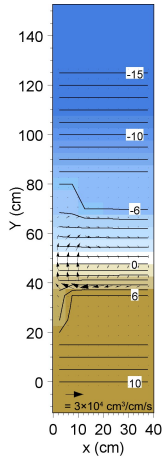

Figure 18. Sand transport flux in Case 7.

6. Reproduction Calculation

6.1. *Application to the results of model experiment*

Because the width of the mouth is one-fourth of the channel width, three-dimensional (3-D) beach changes will occur, so 3-D numerical simulation was carried out. Assuming the initial berm height of 6 cm and the beach slope of 1/5, the calculation domain was discretized by Δx = 5 cm and Δz = 1 cm, and Δt was set as 10^{-4} h. The depth distribution of sand transport was assumed to be a cubic equation given by Uda and Kawano (1996) below MSL and a triangular distribution above MSL with unity at the shoreline and 0 at the berm top. The intensity of sand transport and the equilibrium slope were calculated from Eqs. (11) and (12). Table 3 shows the calculation conditions. The range of $\lambda > 1$ was set to be between x = 0 and 10 cm in the longshore direction, the width of the drainage channel, and the vertical range was determined to be between z = 4 and -5 cm on the basis of the trial and error calculation. λ value in this domain was set to 1.4 and λ was set 1 except this domain. The calculation was carried out by the 100-fold scale, and then the results were reduced by the factor of 1/100.

Figures 17 show the initial bathymetry and calculated bathymetry after a 3-hour wave action for Case 1 without Q_m = 0 and Case 7 with Q_m = 170 ml/s, respectively. In Case 1, shoreward sand transport occurred and sand was deposited near the shoreline with contours densely distributed between -6 cm and 6 cm heights. In Case 7 with Q_m = 170 ml/s, the concave contours on land and the convex contours on the seabed were formed in front of the area with seaward flow. The sand transport flux in Case 7 is shown in Fig. 18. A circulation of sand transport from outside to the area with seaward transport along the shoreline and the return transport in the offshore zone was predicted. Thus, the concave bathymetry in front of the mouth of the floodway could be dynamically maintained, and these results explain the measured topography, as shown in Fig. 4 in front of the Shin-nakagawa floodway. Figure 19 shows the changes in longitudinal profiles in Cases 1 and 7. Although a berm was formed due to the shoreward sand transport in both cases, the berm height in Case 7 was reduced by 2.2 cm compared with that in Case 1, similarly to the experiment.

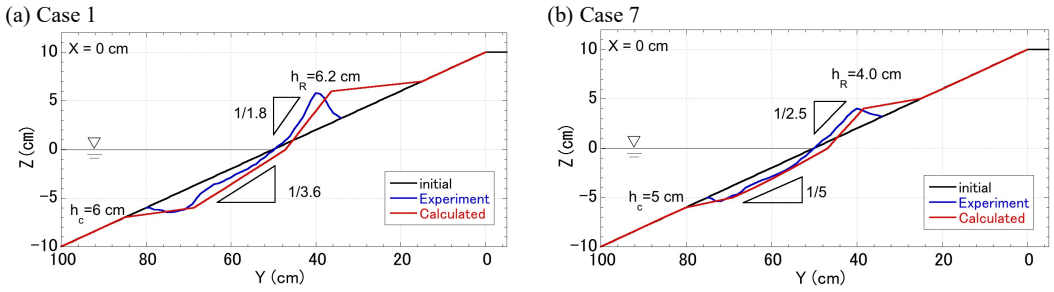

Figure 19. Longitudinal profiles (experiment vs. simulation).

6.2. *Application to the real topography around Shin-nakagawa floodway*

In the vicinity of the Shin-nakagawa floodway, bathymetric survey was carried out in February 2002. Figure 20 shows the bathymetry around the mouth of the old and new floodways. In front of the mouth of the old floodway, a channel connecting to the sea had been formed by the surface flow during a flood. Immediately offshore of this channel, convex contours were formed between 2 and 5 m depth. These combination of the concave shoreline and convex offshore contours is similar to the results in Case 1 shown in Fig. 17, although the seaward flow was triggered by the surface flow. In this application, we included the effect of the seaward flow due to a flood. The discharge of this floodway is approximately 0.8 m^3/s in the normal condition, but the discharge of the floodway increases greater than several m^3/s during a flood. During the flood, seaward sand transport is assumed to be induced by the seaward flow, resulting in the formation of convex contours immediately offshore of the floodway. Figure 21(a) shows the change in longitudinal profile between 2002 and 2013. In the offshore zone deeper than -10 m, offshore sand transport can be observed and sand was deposited up to -32 m because of very steep slope of 1/2, which is equal to the slope of angle of repose of sand. On the shelf with 1/6 slope, both concave profile on the beach and convex profile near the shoreline were formed, as shown in Fig. 21(b).

To reproduce the topographic changes, as shown in Figs. 20 and 21, numerical simulation was carried out given the calculation conditions shown in Table 4. The depth of closure, the initial berm height and the beach slope were set to be 8, 4 m and 1/6, respectively. The calculation domain was discretized by using the meshes of Δx = 5 m and Δz = 1 m. Δt was set to 0.1 hr. As for the wave condition, waves with a breaker height of 1.5 m were assumed to obliquely incident to the direction normal to the shoreline with θ_w = -0.8°. The coefficient of longshore sand transport was 0.037 such that the longshore sand transport of $Q = 1\times10^4$ m^3/yr on this coast occurs. The range of $\lambda > 1$ was set to be between x = -5 and 0 m in the longshore direction, the width of the drainage channel, and the vertical range was set to be between z = 0 and -2 m on the basis of the trial and error calculation. λ value in this domain was determined to be λ = 5 and λ was set to be 1 except this domain. In addition, when the coefficient of cross-shore sand transport was assumed to be $K_z = 0.1K_y$, similarly to the reproduction calculation of the experiment, the longshore width of the protrusion was predicted excessively large compared with the measured. Therefore, $K_z = 0.2K_y$ was selected to enhance the reproduction.

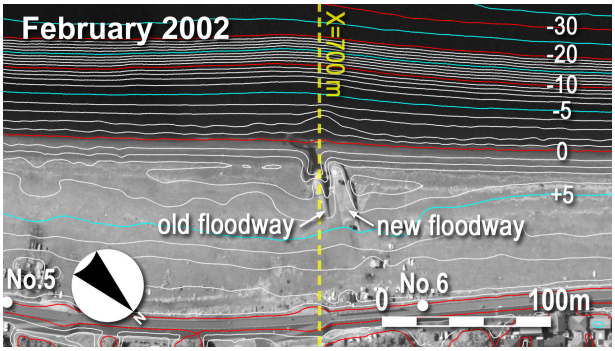

Figure 20. Aerial photograph and bathymetry around Shin-nakagawa floodway in 2002.

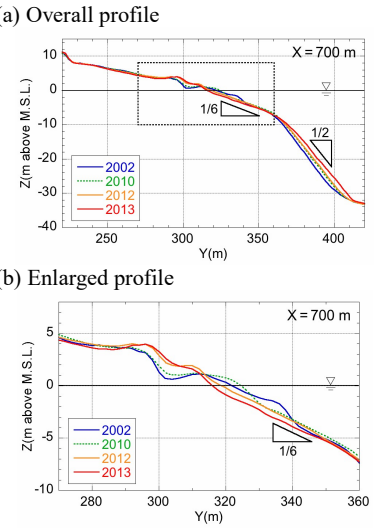

Figure 21. Longitudinal profile in vicinity of floodway.

Table 4. Calculation conditions.

Numerical model	Contour-line change model (Serizawa et al. 2003)
Initial bathymetry	Straight, parallel contours Z = +4 ~ -8 m:1/6 , Z = -8 ~ -32 m:1/2
Equilibrium slope	1/6
Wave conditions	Breaker height H_b = 1.5 m and θ_w = -0.8˚
Depth of closure and berm height	Depth of closure h_c = 8 m, Berm height h_R = 4 m
Coefficients of sand transport	Coefficient of longshore sand transport K_y = 0.037 Coefficient of cross-shore sand transport K_z = 0.2K_y
Depth distribution of sand transport	Cubic equation given by Uda and Kawano (1996)
Critical slope of falling sand	1/2 on land and seabed
Calculation range in depth	z = 4.5 - -32.5 m
Calculation mesh	ΔX = 5 m, ΔZ = 1 m
Time intervals	Δt = 0.1 h
Boundary conditions	q_x = 0 at landward and seaward boundaries, and q_y = 0 at both ends
Remarks	λ = 5 (X = -5 - 0 m, z = 0 - -2 m)

Figures 22(a) and 22(b) show the initial bathymetry of straight, parallel contours, and the results of the prediction. Also, bathymetric changes from the beginning and the change in longitudinal profile are shown in Figs. 22(c) and 22(d). The predicted results are in good agreement with the measured, as shown in Figs. 20 and 21. Finally, Fig. 23 shows the sand transport flux offshore of the floodway. A strong concentrated seaward transport occurred along the centerline of the floodway and a couple of circulation on both sides of the concentrated transport was predicted.

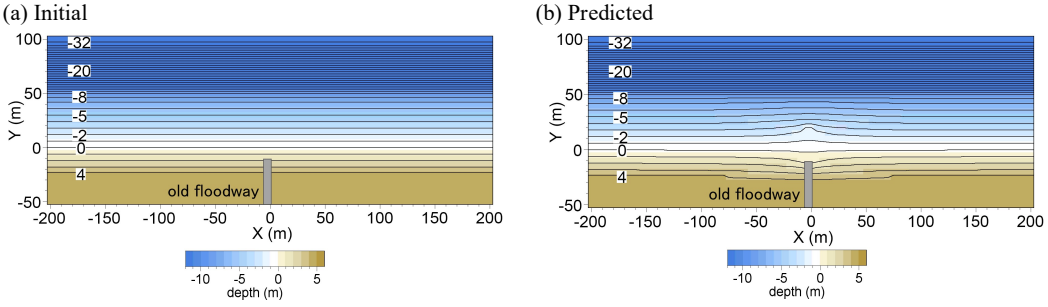

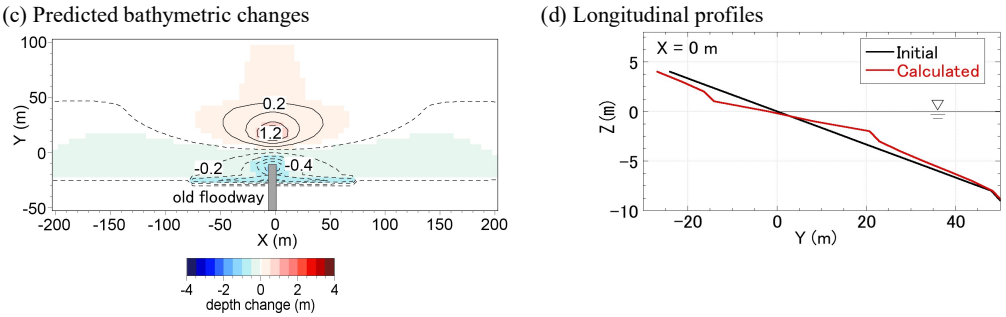

Figure 22. Results of the numerical calculation.

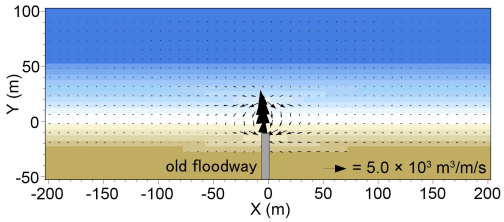

Figure 23. Sand transport flux.

7. Conclusions

In the experiment, gravel with a grain size of 3.3 mm was employed as the material. This grain size can be transformed as 16.5 mm in the prototype. The grain size of the bed material near the Shin-nakagawa floodway ranges from 5 to 10 cm, as shown in Fig. 5, and the grain sizes in the experiment and in the prototype drop in the same order of magnitude, and thus the phenomena observed at the Shin-nakagawa floodway can be explained by the results of the experiment. In the prototype and experiment, the grain size of the bed material is significantly large with a large velocity of the filtration flow. This weakened the wave action during incoming waves, resulting in reductions in the foreshore slope (equilibrium slope) and berm height. The effect of seaward flow originated from filtration on the cross-shore sand transport was incorporated in the contour-line-change model, and calculation results were in good agreement with the experimental results. Furthermore, the model was applied to the calculation of the 3-D bathymetric changes around the Shin-nakagawa floodway caused by the surface flow associated with a flood. The predicted bathymetric changes were in good agreement with the measured.

References

Horikawa, K. ed., 1988. *Nearshore Dynamics and Coastal Processes*, University of Tokyo Press, Tokyo, 522p.

Serizawa, M., Uda, T., San-nami, T., Furuike, K. and Kumada, T., 2003. Improvement of contour line change model in terms of stabilization mechanism of longitudinal profile, *Coastal Sediments '03*, 1–15.

Shibasaki, M., Uda, T., Serizawa, M., Kumada, T. and Kobayashi, A., 2004. On the configuration of rip channel accelerating development of rip current, *Proceedings of 29th International Conference on Coastal Engineering*, ASCE, 1506–1518.

Uda, T. and Kawano, S., 1996. Development of contour-line change model for predicting beach changes, *Proceedings of JSCE*, No. 539/II-35, 121–139. (in Japanese)

Uda, T., Ishikawa, T., Serizawa, M., Serizawa, Okamoto, M., Noshi, Y. and Miyahara, S., 2016. Reductions in berm height and foreshore slope due to filtration flow on gravel beach, Proc. 35th ICCE. (in press).